Atomic Hydrogen in a Magnetic Trapping Field

J.T.M. Walraven, R. van Roijen, and T.W. Hijmans

Natuurkundig Laboratorium, Universiteit van Amsterdam,
Valckenierstraat 65, NL-1018 XE Amsterdam, The Netherlands

We discuss the loading and relaxational decay of spin-up polarized atomic hydrogen (H↑) in a minimum-B-field trap. Our current experiments cover the temperature range from 80 to 225 mK. The maximum obtained density is $n_0 = 3\times10^{14}\,\mathrm{cm}^{-3}$ at $T \approx 100\,\mathrm{mK}$, corresponding to a total of $N = 4\times10^{13}$ atoms. By covering the walls of the sample cell with either pure ^{4}He or with ^{3}He/^{4}He mixtures it could be demonstrated that the stability of the sample is not sensitive for a variation of the surface adsorption energy by as much as a factor 2.5. Measuring the rate at which H↓ is produced in the trap we can accurately determine the dipolar relaxation rate as a function of temperature. We discuss the possibility of optical detection and the prospects for optical cooling of magnetically trapped hydrogen.

I. Introduction

Substantial progress has been made over the last decade in stabilizing atomic hydrogen at high densities but an important goal of the research, the observation of Bose-Einstein condensation (BEC) still is out of reach.[1][2] To observe BEC density-to-temperature ratios $n^{\frac{2}{3}}/T \approx 6.3\times10^{13}\,\mathrm{cm}^{-2}\mathrm{K}^{-1}$ have to be reached. The single important factor that seems to frustrate attempts to satisfy this condition by compressing a sample of spin-down polarized hydrogen (H↓) is the fact that absorption of atomic hydrogen on the helium covered surfaces of the sample cell increases dramatically with decreasing temperature, leading to excessive surface recombination. Currently with H↓, $n^{\frac{2}{3}}/T \approx 5\times10^{12}\,\mathrm{cm}^{-2}\mathrm{K}^{-1}$ has been reached.[3][4][5][6] It was suggested by Hess that a possible way around this problem would be to eliminate the influence of surfaces altogether by trapping a gas of spin-up polarized hydrogen (H↑) in a static magnetic-field minimum.[7]

The absence of surface effects may be very appealing, but a serious disadvantage of trapping in a B-field minimum is that the gas phase of H↑ is much less stable than that of H↓. For densities where three-body effects are negligible the stability of H↓ is limited by nuclear dipolar spin relaxation, opening up a path to the molecular state H_2. The stability of H↑ is determined by electronic dipolar spin relaxation to the high-field seeking hyperfine states, which are ejected from the trap. This dipolar relaxation process limits the attainable densities of H↑ in the trap to about $10^{14}\,\mathrm{atoms/cm}^3$. With H↓, densities exceeding $10^{18}\,\mathrm{cm}^{-3}$ have been reached.[3-6] The real challenge of the trapping experiments is therefore the attainment of ultra-low temperatures in order to satisfy the BEC requirements. For a density $n = 10^{14}\,\mathrm{cm}^{-3}$ the gas should be cooled to a temperature below 34 μK.

The Hydrogen Atom Editors: G.F. Bassani · M. Inguscio · T.W. Hänsch

The feasibility of surface-free confinement of H↑ was recently demonstrated by Hess et al.(MIT), who reported trapping of up to 5×10^{12} atoms and temperatures as low as $T=40$mK ($n^{\frac{2}{3}}/T\approx1\times10^{10}\mathrm{cm}^{-2}\mathrm{K}^{-1}$).[8] These authors fire a sub-kelvin discharge after which a mixture of four hyperfine states is present in the trapping region. We use the labels *a*, *b*, *c* and *d* for the hyperfine states of H in its electronic ground state in order of increasing energy. Within a second, the field gradients lead to spatial separation of H↑ (a mixture of the *c* and *d* states) and H↓ (a mixture of the *a* and *b* states). The trapping of the H↑ results from interatomic collisions in which potential energy due to the trapping potential is converted into kinetic energy which is carried off by the walls of the sample cell. By allowing hot atoms to escape from the trapping region Hess et al. demonstrated that the gas could be cooled to a temperature well below the wall temperature. This technique is known as evaporative cooling.[7] To study the gas, Hess et al. measured the number of atoms remaining in the trap after a certain holding time by dumping the content of the trap onto a magnetic resonance detector.

In this paper we describe an experiment in which we study the loading and relaxational decay of H↑ in a minimum-*B*-field trap.[9] In our geometry, evaporative cooling is absent. The trap is filled with a pure H↑-flux until a steady state is reached. We monitor the H↑ continuously during (and after) filling by observing the atoms ejected from the trap towards high field after magnetic relaxation. The principle of this experiment and a description of the apparatus is presented in section II. The results are discussed in section III. In section IV we address the prospects of magnetic trapping of H↑. In particular we speculate on the use of an optical method to study and cool a gas of trapped H↑.

II. The experiment

The principle of our experiment is illustrated in Fig.1, where we show a block diagram of the experimental cell as well as the effective trapping potential along the symmetry axis ($r=0$; dashed curve). This curve reflects the magnetic trapping field but also includes the surface adsorption potential due to the wall at the left side of the cell. The solid line corresponds to the field at the wall of the sample cell ($r=6.5$mm). Our trap has a depth equivalent to $\epsilon_{tr}/k_B=0.92$ K. This depth is somewhat smaller than the binding energy of H on the surface of liquid ^{4}He, $\epsilon_a/k_B\approx1$ K,[10] and much larger than the binding energy on a ^{3}He/^{4}He mixture, $\epsilon_a/k_B\approx0.4$ K.[11] The H atoms are produced in high field in a dissociator operated at a temperature $T\approx600$mK. The low field seeking atoms (H↑) are guided through a capillary to the trapping volume which encloses the *B*-field minimum but also extends to the high field zone. All surfaces are covered with a film of liquid helium. The H↑ atoms, entering the cell thermalize with the walls and fill the trap. These atoms cannot escape the low field region due to the presence of walls

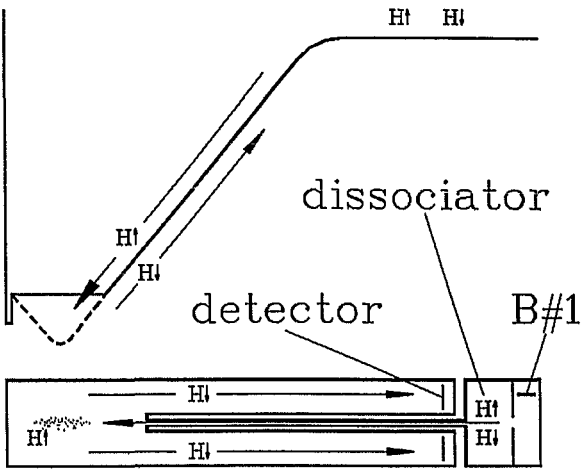

Fig.1. *Principle of the experiment. The low field seeking atoms are driven to the B-field minimum. The gas is studied by observing the atoms that escape the trap after relaxation*

and the high field barrier. The H↓ atoms produced in the discharge tend to stay in the dissociator region where they are sorption pumped by a helium-free bolometer chip (B#1). Similarly, H↓ atoms spuriously entering the cell are continuously sorption pumped by a helium free bolometer plate ('pumping plate'[12][13]) positioned at the high-field end of the sample cell. To study the trapped H↑ we observe the H↓ atoms which are ejected from the trap as a result of magnetic relaxation in the H↑ sample. The dominant relaxation processes are spin exchange and magnetic dipolar relaxation of the electron spins.[14] As spin exchange is very fast but only occurs in *c-c* collisions (*cc→aa*, *ac*, *bd*) it leads to preferential depletion of the *c* states, leaving the gas in the *d* state which is doubly polarized.[14] By properly choosing the dimensions of the experimental cell we could achieve that essentially all of the relaxing atoms arrive at the detector.

The experimental cell is shown in Fig.2. For dissociation we use a compact and rugged $\frac{1}{4}\lambda$ helical cavity with a $Q \approx 300$, resonating at 718 Mhz and driven with 0.1 W × 50 μs pulses at a 50 Hz repetition rate. The method of RF dissociation at low temperatures was pioneered by Hardy et al.[15] and discussed extensively by Helffrich et al.[16]. The bolometer B#1, used to remove H↓ fraction trapped in the dissociator region, is mounted in a separate volume connected to the dissociator volume by a 1 mm diameter drilled hole. The dissociator operates optimally at $T \approx 600$mK and can produce an H↑ flux of up to 5×10^{12}/s which is guided to the trapping volume through a thin-walled german silver (GS) tube (3.6 mm i.d.). Thermometry is done against a ^{3}He melting line thermometer. The temperatures of cell and dissociator may be varied independently. The 'pumping plate' is mounted in the annular part at the lower end of the cell. This part is positioned in high field ($B \approx 4$ T). The plate

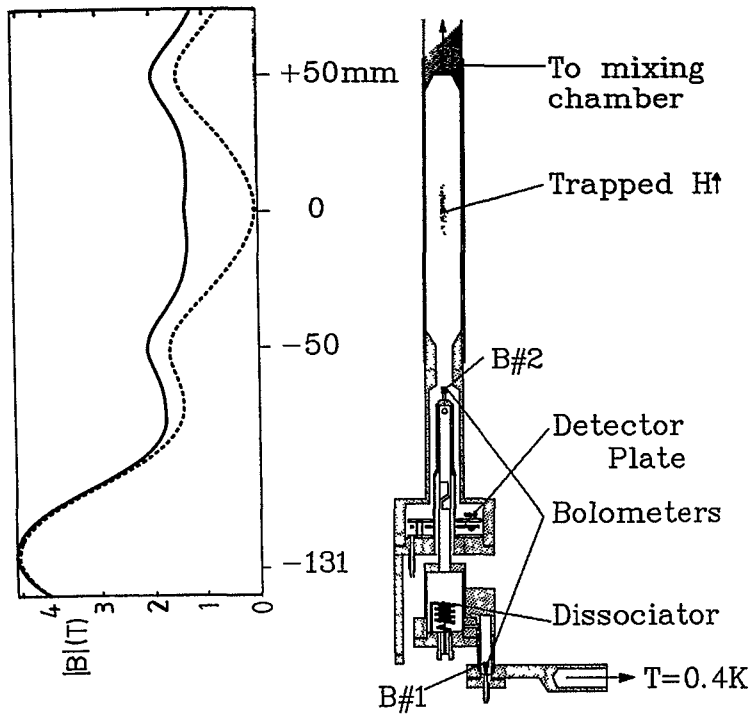

Fig.2. *Drawing of the experimental cell. On the left we show the magnetic field profile for both the symmetry axis (dashed curve) and for a distance of 6.5 mm from the axis*

has an area of 3.5 cm^2 and is suspended by three 16 μm tungsten wires. The assembly requires 20 μW to boil off the helium film and is stabilized at $T = 1.4$ K. The minimum detectable flux is 2×10^{11} at/s. The detector efficiency is approximately 60% of the recombination heat.[17] A second bolometer (B#2) is mounted on top of the end cap of the GS filling tube, located in the fringe field of the trap. This bolometer enables us to trigger recombination of the gas in the trap.

The trapping field is similar to that discussed by Pritchard [18] and Hess[7] and is generated by a superconducting coil system operated during the measurements in persistent mode. For radial confinement we use four racetrack shaped coils which provide a quadrupole field. At maximum current (36 A) the quadrupole field reaches 1.4-1.5 Tesla at $r = 6.5$ mm, the surface of the sample cell. Two dipole fields are used for axial confinement. They are located near the ends of the racetracks at $z = +50$ mm and $z = -50$ mm with respect to the center of the trap. These coils produce fields of 1.7 and 1.5 Tesla respectively. The B-field minimum may be adjusted between $B = 0$ to $B = 1$ T with a trim coil incorporated at $z = 0$. At the lower end of the racetracks we mounted a 4.4 T dipolar coil at $z = -131$ mm

which serves to separate H↑ and H↓. In Fig.2 we also show the field profile of our trap for both $r = 0$ (dashed curve; cell axis) and $r = 6.5$ mm (solid curve; cell wall).

A typical measurement cycle is shown in Fig.3. During the full cycle both bolometer B#1 and the pumping plate are actively pumping H↓. At $t = -62$ s the dissociator is switched on and the film is removed from B#2. Hence no H↑ density can build up in the trap. The flux observed to appear rapidly is caused by H↓ spuriously entering the cell as was verified by varying the B-field in the dissociator region and changing the temperature of the GS filling tube. At $t = -50$ s B#2 is switched off and the trap starts to fill as witnessed by the slowly growing flux escaping the trap region. When the dissociator is switched off at $t = 0$, H↓ keeps emerging from the cell during 50 seconds after which the remaining H↑ is removed by reactivating B#2. This procedure ensures a proper zero flux base line for the data analysis. We start the analyses at $t = 2$ s when the spurious H↓ signal is known to have disappeared as could be established by keeping B#2 activated during a full cycle.

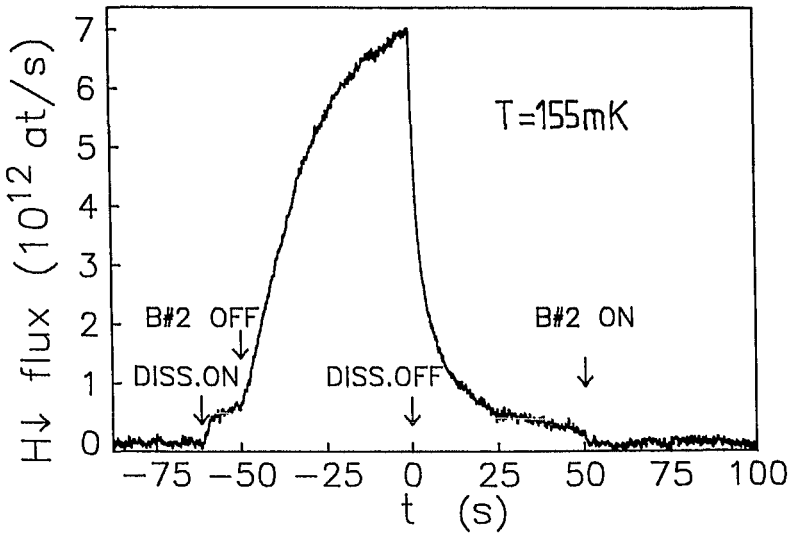

Fig.3. *Observed hydrogen flux versus time (raw data). For discussion see text*

To study the relaxation of H↑ to the high field seeking hyperfine states we plot our data as $V_\gamma \dot{N}/N^2$ versus time as shown in Fig.4. $N(t)$ is the total number of atoms in the trap at a given time t, obtained by integrating the observed flux $\dot{N}$ from t to ∞. V_γ is the effective volume of the sample defined by $V_\gamma = V_{1e}^2/V_{2e}$, where $V_{me} = \int (n(\vec{r})/n_0)^m d\vec{r}$. The density of the sample at the center of the trap is given by n_0. For our trap $V_\gamma T_g^{-\frac{5}{2}} \approx 180\ \mathrm{cm^3 K^{-\frac{5}{2}}}$. In plotting the data we set the gas temperature T_g equal to the wall temperature T_w. For temperatures above 100 mK the

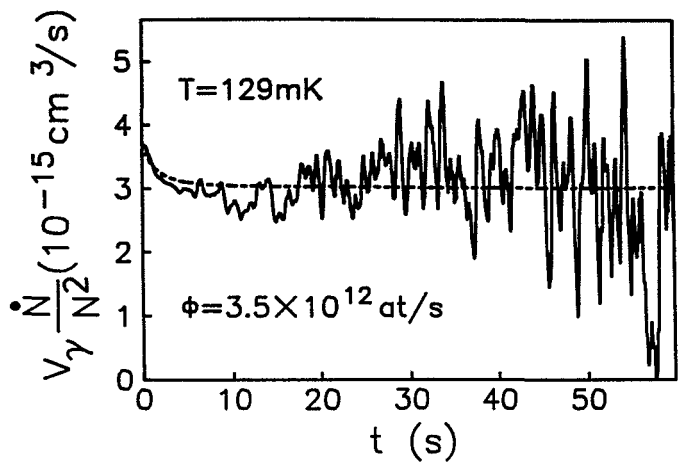

Fig.4. *Typical decay curve plotted as* $V_\gamma \dot{N}/N^2$ versus time; ϕ *is the H↑ filling flux and the dashed line represents a simulation*

initial decay tends to be faster than the decay expected for dipole-dipole relaxation alone. This enhanced initial decay (EID) is observed during up to 8 s after switching off the discharge. As discussed below, this effect is attributed to spin-exchange relaxation and nuclear polarization. For $T < 100$ mK a reduced initial decay (RID) is observed for up to 15 s. The RID is attributed to loss of thermal contact between gas and cell walls.

Using the theoretical results of Stoof et al.[19] we calculate $\dot{N}(t)$ by averaging the field and temperature dependent relaxation rates over a thermal density distribution. The contribution due to an individual process may be written as

$$\dot{N} = (\gamma_0 G_0 / V_\gamma) N_{h1} N_{h2} \qquad (1)$$

where G_0 is the rate constant of the process, evaluated for the conditions at the center of the trap, and $\gamma_0 \equiv \int \{G(\vec{r})/G_0\}(n(\vec{r})/n_0)^2 d\vec{r}/V_{2e}$ includes all effects due the field dependence of the rate. The effective volume V_γ accounts for all effects associated with the spatial distribution of the gas. N_{hi} refers to the total number of atoms in the trap in hyperfine state *hi*. The correction factor γ_0 varies substantially with temperature. For T_g increasing from 80 to 225 mK, γ_0 increases from 2.1 to 3.5 for the dipolar relaxation processes. For spin exchange, γ_0 decreases from 0.28 to 0.08 in this temperature range. Calculating the decay curves we find that the dominance of the spin exchange terms in the rate equations leads to nuclear polarization and to an EID-period after which the polarization reaches a steady state. In Fig.4 the calculated EID denoted by the dashed curve. We find that the asymptotic decay is described to within 3% by $V_\gamma \dot{N}/N^2 = \gamma_{dd} G_{dd}$, where $G_{dd} \equiv 2G^d_{ddaa} + G^d_{ddac} + G^d_{ddad}$ in the notation of ref.[14].

III. Results

In our experiments densities up to $n_0 = 3\times10^{14}\,cm^{-3}$ were reached at the center of the trap for $T \approx 100$mK. This corresponds to a total of $N = 4\times10^{13}$ atoms. The results for the dipole-dipole relaxation rate are given in Fig.5. The data points represent the overall second order decay rate $\gamma_0 G_0 = V_\gamma \dot{N}/N^2$ versus T obtained from plots like Fig.4 by discarding the EID/RID-period of 15 s. The open circles refer to data taken with ^{4}He covered surfaces. The data represented by solid circles were taken after 1% ^{3}He was added to the cell. For ^{4}He surfaces the measurements extend over a temperature range from 135 mK to 225 mK. The lower limit is caused by a lack of filling flux due to surface recombination in the filling tube. Above 225 mK the H↑ density near the detector plate becomes non-negligible and gives rise to systematic errors due to recombination of H↑ on the detector. With ^{3}He in the cell the detector was found to be unreliable for $T > 160$ mK due to heat conduction by the ^{3}He vapor. At the lower end of the temperature range we were limited by the cooling power of our dilution refrigerator.

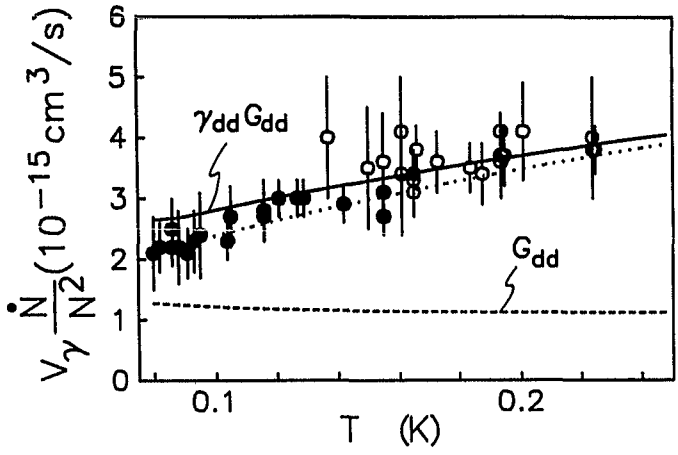

Fig.5. *The second order decay rate plotted versus temperature* (○: ^{4}*He wall coverage*; ● ^{3}*He/*^{4}*He coverage*). *Dashed line*: *theoretical result for the bottom of the trap*. *Solid line*: *including the field average*. *Dotted line*: *see text*

We find good overall agreement with the theoretical curve for $\gamma_{dd}G_{dd}$ (solid curve in Fig.5). Hence our data reflect the strong temperature dependence of V_γ. From this we infer that the gas in the trap is thermalized to the wall temperature. The slight deviation of the data with respect to the solid curve below 100 mK could in principle be explained by assuming T_g to be 8mK higher than T_w as illustrated by the dotted curve in Fig.5. However, this effect could also be accounted for by a 17% systematic error, not included in the error bars, related to the limited calibration accuracy of the detector. Comparing the open and closed circles one observes that the relaxation rate is insensitive for the surface

coverage, as is to be expected for $\epsilon_{tr} \geq \epsilon_a$. The dashed curve represents G_{dd} for $B = 0.05$ T and shows the small intrinsic temperature dependence of the dipolar rate. From a comparison of our data with the solid and dashed curves we infer that our results confirm the increase of the dipolar rate with growing field predicted by theory. Also the experimentally observed increase of the relaxation rate with increasing temperature reflects this behavior. Dividing our data by γ_{dd} we find $G_{dd} = 1.1(2) \times 10^{-15} cm^3/s$ for $T = 100$ mK and $B = 0.05$ T. This is more accurate than the result of Hess et al.[8] and in good agreement with the theoretical value $G_{dd} = 1.2 \times 10^{-15} cm^3/s$.[19]

The observed RID's can be explained if we assume that just after switching off the discharge, the gas is at a slightly higher temperature ($\Delta T < 10$ mK) than the walls and cools down to T_w in 10-15 s. Even a small ΔT should show up as a substantial RID due to the strong temperature dependence of V_γ. However, on the basis of a computer simulation of the decay we expect an exponential temperature dependence of the thermal accommodation time. This is not in line with the measurements, moreover the observed RID's are larger than we expect. This point deserves further study.

IV. Prospects

Even for the relatively high density $n_0 = 3 \times 10^{14} cm^{-3}$ obtained at the center of our trap at $T \approx 100$ mK we are far from BEC. The density-to-temperature ratio for these conditions is $n^{\frac{2}{3}}/T \approx 4.5 \times 10^{10} cm^{-2} K^{-1}$, which is still two orders of magnitude lower than the value obtained by compressing H↓. Therefore the temperature has to be reduced by three orders of magnitude to reach BEC. On the basis of our present results we estimate that our current technique is applicable down to approximately 55 mK. To achieve lower temperatures we are developing a Lyman-α (L_α) optical cooling method. Since this leaves the number of particles intrinsically unaffected high densities should be attainable at temperatures below 10 mK. The optical approach is also very attractive from the point of view of detection and thermometry since it is both extremely sensitive and non-destructive.

We briefly describe our optical plans. Fig.6 shows the hyperfine structure of

TABLE 1
Recoil effects.

recoil velocity: $\delta v = (\hbar\omega/mc)$
recoil energy: $E_r = \frac{1}{2}m(\delta v)^2$ (v=0)
frequency shift: $\delta\omega/\omega = (v/c)\cos(\vec{k},\vec{v}) + \frac{1}{2}\delta v/c$
thermal velocity: $\bar{v} = (8kT/\pi m)^{\frac{1}{2}}$

$\bar{v}$ is given for T=50mK

$\delta v/\bar{v} = (\hbar\omega/c)(\pi/8mkT)^{\frac{1}{2}}$
$\delta\omega/\omega = \frac{1}{2}\delta v/c$ (v=0)

	δv (m/s)	$\bar{v}$ (m/s)	$\delta v/\bar{v}$ (%)	$\delta\nu$ (MHz)	E_k/k_B (mK)
H	3.25	32.4	10.0	13.5	0.64
D	1.63	22.9	7.1	6.8	0.32
^{23}Na	0.03	6.7	0.4	25kHz	0.0012

the 1S, 2S and 2P manifolds of the hydrogen atom. In a minimum-*B*-field trap only atoms in the low field seeking hyperfine states are present, primarily the *d* state. For temperatures below 20 mK thermometry is probably best done by measuring the ratio of the intensities of the π_1 and σ_1 lines. At present it is hard to assess the limitations of this method but accurate thermometry in the 10-100 μK regime should be feasible.

Recoil effects, when absorbing or emitting L_α, are extraordinary large in hydrogen as a direct result of the small mass of the atom and the large momentum of the Lyman-α photon. This is illustrated in Table 1 for absorption events with maximum momentum transfer. The large recoil makes it fascinating to analyze the prospects for optical cooling H↑ (or D↑) in the minimum-*B*-field trap. To cool the gas in our trap optically one has to tune to the low frequency wing of the

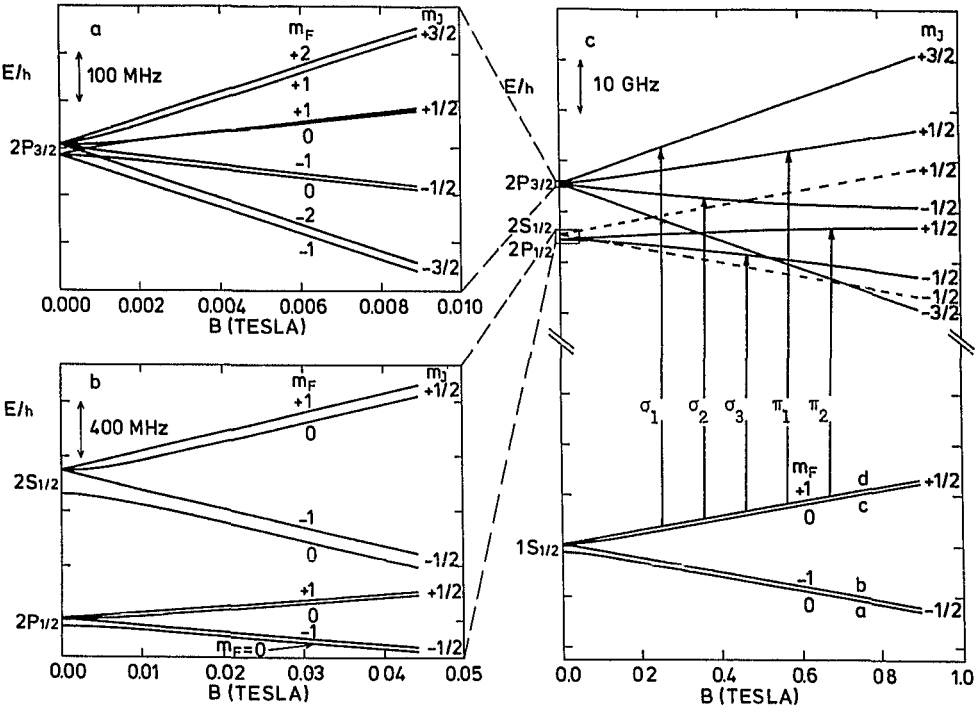

Fig.6. *The hyperfine structure of the 1S, 2S and 2P manifolds of the H-atom. We also show the transitions from the d-state which are allowed within a fine-structure picture*

transition to the $2^2P_{\frac{3}{2}}(m=\frac{3}{2})$ level (σ_1). This state decays back only to the *d* state. To evaluate the cooling efficiency let us assume the trap to be loaded with a total of 10^{10} atoms at 80 mK ($n_0 = 7\times10^{11}cm^{-3}$), a condition at which the intrinsic lifetime of the sample is of order hours. From Table 1 one observes that only 10 absorption events with maximum momentum transfer are needed to 'stop' an H-atom.

For our trap, where the atoms are moving in random directions and experience a spatially varying magnetic field, a computer simulation showed that about 80 photons/atom are needed to cool to below 10mK. Assuming a photon flux of 10^{11}-10^{12}photons/s temperatures below 10 mK can thus be reached well within 10 s. The required intensities (5×10^{8}photons/pulse; 100 Hz repetition rate) and band widths (100 MHz) are state of the art in VUV generation.[20][21]

To reach BEC one has to cool beyond the optical quantum limit $\frac{1}{2}\hbar\Gamma/k_B = 2.2$mK for H. Here Γ is the natural line width of the L_α transition. For this an evaporative cooling scheme seems to be indispensible. Apart from the procedure suggested by Hess [7] in which the trapping fields are lowered, the evaporation may also be induced by optical pumping to one of the high-field-seeking ground state hyperfine levels. For this purpose the σ_2 or π_2 transitions could be used. Also magnetic resonance may be used to induce evaporation. A preliminary analysis has shown that this type of evaporation can be as efficient as the method proposed by Hess.

In the final stage of the preparation of this manuscript we received a preprint from Masuhara et al.[22] reporting $n_0 = 7.6\times10^{12}\mathrm{cm}^{-3}$ at $T = 3$ mK ($n^{\frac{2}{3}}/T \approx 1.3\times10^{11}\mathrm{cm}^{-2}\mathrm{K}^{-1}$), obtained by evaporative cooling.

V. Acknowledgements

The authors benefitted from many useful discussions with the Eindhoven theory group of B.J. Verhaar and the group of A.Lagendijk. The trapping experiments were done in collaboration J.J. Berkhout and S. Jaakkola. This work is part of the research program of the 'Stichting voor Fundamenteel Onderzoek der Materie (FOM)', which is financially supported by the 'Nederlandse Organisatie voor Wetenschappelijk Onderzoek (NWO)'.

References

1. I.F.Silvera and J.T.M.Walraven, Progr.Low Temp.Phys. edited by D.F.Brewer (North-Holland, Amsterdam, 1986), Vol X, 139.
2. T.J. Greytak and D. Kleppner, New Trends in Atomic Physics, edited by G.Grynberg and R.Stora (Elsevier, Amsterdam, 1984), Vol.II, 1125.
3. R.Sprik, J.T.M.Walraven, and I.F.Silvera, Phys.Rev.B 32, 5668 (1985).
4. D.A.Bell, H.F.Hess, G.P.Kochanski, S.Buchman, L.Pollack, Y.M.Xiao, D.Kleppner, and T.J.Greytak Phys.Rev.B 34, 7670 (1986).
5. T.Tommila, E.Tjukanov, M.Krusius, and S.Jaakkola, Phys.Rev.B 36, 6837 (1987).
6. J.D.Gillaspy, I.F.Silvera, and J.S.Brooks (1988), to be published.
7. H.F. Hess, Phys.Rev.B(RC) 34, 3476 (1986).
8. H.F.Hess, G.P. Kochanski, J.M. Doyle, N.Masuhara, D.Kleppner, and T.J.Greytak, Phys.Rev.Lett. 59, 672 (1987).
9. R.van Roijen, J.J.Berkhout, S.Jaakkola, and J.T.M.Walraven, to be published.
10. For a compilation of measurements of the binding energy of H on ^{4}He see W.N. Hardy, M.D. Hürlimann, and R.W. Cline, Jap.J.Appl.Phys. 26, 2065 (1987) suppl. 26-3 (LT18).
11. G.H. van Yperen, A.P.M. Matthey, J.T.M. Walraven, and I.F. Silvera, Phys.Rev.Lett. 47, 800 (1981).

12. J.J.Berkhout, O.H.Höpfner, E.J.Wolters, and J.T.M.Walraven, Jap.J.Appl.Phys. 26, 231 (1987) suppl. 26-3 (LT18).
13. J.J.Berkhout, E.J.Wolters, R.van Roijen, and J.T.M.Walraven, Phys.Rev.Lett. 57, 2387 (1986).
14. A.Lagendijk, I.F.Silvera en B.J.Verhaar, Phys.Rev.B (RC) 33, 626 (1986).
15. W.N.Hardy, M.Morrow, R.Jochemsen, B.W.Statt, P.R.Kubik, R.M.Marsolais, and A.J.Berlinsky, Phys.Rev.Lett. 45, 453 (1980).
16. J. Helffrich, M. Maley, M. Krusius, and J.C. Wheatley, J.Low Temp.Phys. 66, 277 (1987).
17. J.J.Berkhout, O.H.Höpfner, E.J.Wolters, and J.T.M.Walraven, Jap.J.Appl.Phys. 26, 231 (1987) suppl. 26-3 (LT18).
18. D.E.Pritchard, Phys.Rev.Lett. 51, 1336 (1983). V.S.Bagnato, G.P.Lafyatis, A.G.Martin, E.L.Raab, R.N.Ahmad-Bitar and D.E.Pritchard, Phys.Rev.Lett. 58, 2194 (1987).
19. H.T.C.Stoof, J.M.V.A.Koelman, B.J.Verhaar (1988), to be published and private communication.
20. S.Chu, A.P.Mills, A.G.Yodh, K.Nagamine, Y.Miyake, and T. Kuga, Phys.Rev.Lett. 60, 103 (1988).
21. R.Hilbig and R.Wallenstein, IEEE J.Quantum Electron. 15, 1566 (1981).
22. N. Masuhara, J.M. Doyle, J.C. Sandberg, D. Kleppner, T.J. Greytak, H.F. Hess and G.P. Kochansky, to be published.